

## Crystallographic preferred orientations analysis of quartz crystals in Psammite using electron backscatter diffraction, western Ireland

Aziz Rahimi-Chakdel

Department. of Geology, Faculty of Sciences, Golestan University, Gorgan, IRAN

e-mail: a.rahimi@gu.ac.ir

(received: 27/01/2014 ; accepted: 06/07/2014)

### Abstract

The present study investigates the crystal preferred orientation (CPO) of quartz crystals in psammitic rocks to ascertain the deformation mechanism using electron backscatter diffraction (EBSD) on quartz crystals from north of the Renvyle-Bofin Slide (RBS) near Letterfrack in western Ireland. Complete crystallographic orientations were determined for several thousand individual quartz crystals in psammite samples to provide a dataset for exploring the active deformation mechanism(s). Quartz crystallographic orientations are plotted as pole figures and contour diagrams in  $\langle 0001 \rangle$  and  $\langle 11\ 20 \rangle$  directions. Quartz-c-axis patterns show maxima in the Y axis of the pole figure, which can be explained by the dominance of prism  $\langle a \rangle$  gliding, indicating that dislocation creep was the dominant deformation mechanism.

**Keywords:** Quartz crystals, Crystal preferred orientations, Deformation mechanism, Electron backscatter diffraction

### Introduction

The analysis of crystallographic preferred orientation patterns (CPOs or textures) is of considerable interest for the investigation of the structural evolution of tectonic units. CPO development is governed by the following factors: 1. the active deformation mechanism; 2. the shape of the finite strain ellipsoid (plane strain, oblate or prolate) and the strain magnitude; and 3. the strain path.

Texture analysis has become an important tool in evaluating deformation processes as it provides critical information on deformation mechanisms and conditions, finite strain, paleostress and kinematics (e.g., Law, 1990; Schmid, 1994; Leiss *et al.*, 2000; Unzog & Kurz, 2000; Lebit *et al.*, 2002; Rahimi-Chakdel *et al.*, 2006; Bestmann *et al.*, 2011).

The crystallographic preferred orientations of minerals such as quartz can be completely quantified by the methods of electron backscatter diffraction (EBSD), resulting in distribution functions that reveal active slip systems and strain symmetries, as well as asymmetries with macroscopic strain features indicating shear sense (e.g., Wenk, 1985; Schmid & Casey, 1986; Bestmann *et al.*, 2011).

Many researchers (Brunel, 1980; Klaper, 1988; Law, 1990; Passchier & Trouw, 1996; MacCready, 1996) suggest that quartz textures might represent the final late increments of deformation in rock. This raises questions about the relationship

between crystallographic preferred orientations of minerals and their grain shape orientation, which potentially corresponds to the stretching direction. For instance, such lineation could be formed by quartz grains or aggregates elongated in the foliation plane, which is generally interpreted as a stretching fabric parallel to the X-axis of the finite strain ellipsoid. Quartz commonly occurs as a main matrix phase in such metamorphic rocks. Textures defined by quartz in the matrix have been widely used to investigate textural development. In this study, I investigate the potential of electron backscatter diffraction (EBSD) to develop understanding of texture formation, and also to test some of the assumptions generally inherent in textural interpretation.

This study discusses the significance of crystallographic preferred orientations (CPOs) of quartzes. The kinematic significance of CPOs is well-documented and understood for deformed quartz-bearing rocks (Tullis, 1977; Schmid & Casey, 1986; Law, 1986, 1990; Rahimi-Chakdel *et al.*, 2006) in garnet schist and for quartz inclusions in garnet (Jiang *et al.*, 2002), so that an analysis of quartz crystals using more accurate tools should potentially provide a record of the kinematic history during deformation.

### Geological setting and temperature conditions

The sample was collected from Connemara, Ireland. Connemara is one of the best dated segments in the Caledonian-Appalachian Orogen

and differs from the North Mayo Dalradian in that the metasedimentary rocks are intruded by a number of early-mid Ordovician age gabbros and quartz diorites (Leake, 1989). The Connemara Dalradian can be interpreted as both the deformed margin of Laurentia and the mid-crustal roots to a syn-collisional volcanic arc (e.g., Yardley *et al.*, 1982). Following peak metamorphism in the Connemara Dalradian, radiometric dating indicates that the orogen experienced rapid cooling ( $>35^{\circ}\text{C}/\text{m.y.}$ ; Friedrich *et al.*, 1999a, b), typically explained as a response to orogenic collapse. Power *et al.* (2001) used fluid inclusion techniques to estimate rates of exhumation in Connemara of at least 7 km in 10 m.y., similar to modern massifs that exhibit the fastest exhumation rates. Clift *et al.* (2004) have explored the exhumation and orogenic collapse of the Irish Dalradian and assess its implications for the tectonic evolution of this area and for the process of arc-continent collision. In Connemara, exhumation is also achieved by synchronous thrusting and detachment faulting that combines to extrude deeply buried metasedimentary rocks to the surface (Clift *et al.*, 2004). A key feature of all major detachment systems is the presence of a significant metamorphic contrast with low-grade rocks in the hanging wall and higher-grade exhumed rocks in the footwall. Across Clew Bay, a clear difference in grade has long been recognized between the low-grade South Mayo Trough and the higher-grade Dalradian in North Mayo. Much of the contact is covered by Silurian and Carboniferous sedimentary rocks, except on the island of Achill Beg, located in north-west Clew Bay, where a major high-angle fault, the Achill Beg Fault, places the accretionary complex sedimentary rocks of the Clew Bay Complex under the youngest Dalradian rocks seen in the North Mayo inliers of the upper Argyll Group (Chew, 2003). Wellings (1998) proposed that extension along an east-west trending, north-dipping tectonic discontinuity through northern Connemara, known as the Renvyle–Bofin Slide (RBS), was responsible for exhumation of the main Dalradian of the Twelve Bens, whereas Williams and Rice (1989) favoured a role for low-angle extensional faults south of Connemara. Although the Renvyle–Bofin Slide is a major extensional structure, it is not considered to be the master structure because no major metamorphic break is observed across it (Clift *et al.*, 2004). Because of

the strike-slip emplacement of South Connemara, it is possible that the original root zone of the detachments was not preserved within this block or has been buried by later sedimentation (Clift *et al.*, 2004). By comparison with North Mayo, a detachment might be expected to separate high-grade rocks in Connemara from a lower grade arc rocks towards the south, similar to the model proposed by Williams and Rice (1989).

To the south of the RBS is found part of the classic continental shelf Dalradian stratigraphy of the Argyll Group (Fig. 1): the Bennabeola Quartzite, Streamstown and Lakes Marble Formations, which comprise quartzites, psammities, pelites, semi-pelites, amphibolites and marbles (Boyle & Dawes, 1991). To the north is a monotonous sequence of psammities, semi-pelites and rare pelites (locally called the Kylemore Formation, shown in Fig. 1) that was intruded by a series of ultrabasic and basic igneous bodies, the Dawros-Currywongaun-Doughruagh Complex (DCDC). Original bedding is much less clear in the Kylemore Formation. Around the DCDC, rocks north of the RBS are sillimanite-bearing and record metamorphic temperature of up to  $880^{\circ}\text{C}$  (Boyle & Dawes, 1991). These rocks are characterized by a pronounced north-plunging stretching lineation, which seems to be related to the bend in the RBS to the west of the DCDC coupled with transpressional, sinistral strike-slip motion on the RBS (Fig. 1) (Boyle & Dawes, 1991).

### Structure

The RBS juxtaposes the Kylemore Formation against Bennabeola quartzites (Fig. 1). The Bennabeola quartzite in contact with the RBS shows evidence of strong mylonitization in a  $<1$  metre wide zone. The mylonitic fabrics are cut through by brittle dislocations oriented parallel to the general strike of quartzite. Angular fault breccias of disoriented mylonitic quartzite fragments and blocks up to 15 cm across set in a matrix of finer crushed mylonitic quartzite are locally developed along the brittle dislocations, indicating brittle deformation after ductile deformation along the RBS (Boyle & Dawes, 1991). The most obvious macroscopic structures in the Kylemore Formation psammities sample from north of the RBS are well-developed foliation and lineation structures (Fig. 2). The foliation is defined mainly by the parallel alignment of phyllosilicate

minerals, but also by quartz and feldspar in more psammitic lithologies. North of the RBS, the foliation shows much greater variation in strike, especially inside the sillimanite isograd. The lineation is defined mainly by the parallel

alignment of elongated quartz and feldspar crystals. The strike/dip of foliations and trend-plunge of lineation fabrics are plotted on stereographic projections (Fig. 3).

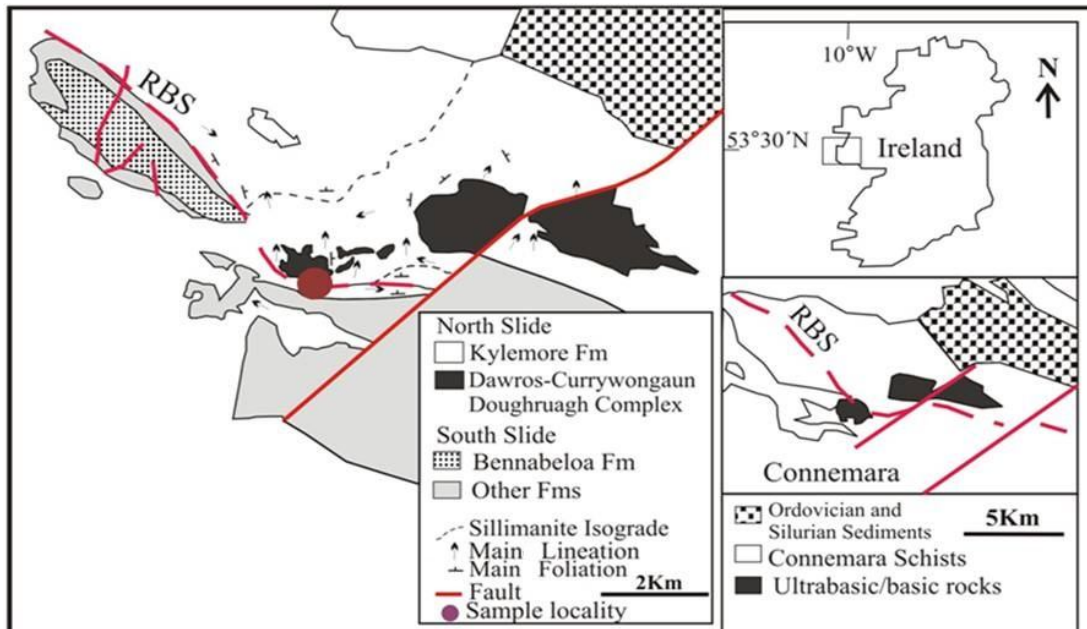


Figure 1: Geological sketch map of studied area (slightly modified from Boyle & Dawes 1991). In the North RBS, the Kylemore Formation contains psammities, semi-pelites and rare pelites. The Dawros-Currywongaun-Doughruagh Complex (DCDC) includes a series of ultrabasic and basic igneous bodies. To the south of RBS, The Bennabeola Quartzite, Stremstorm and Lakes Marble Formations comprise quartzites, psammities, pelites, semi-pelites, amphibolites and marbles. The samples' localities are shown as red circles on the map.

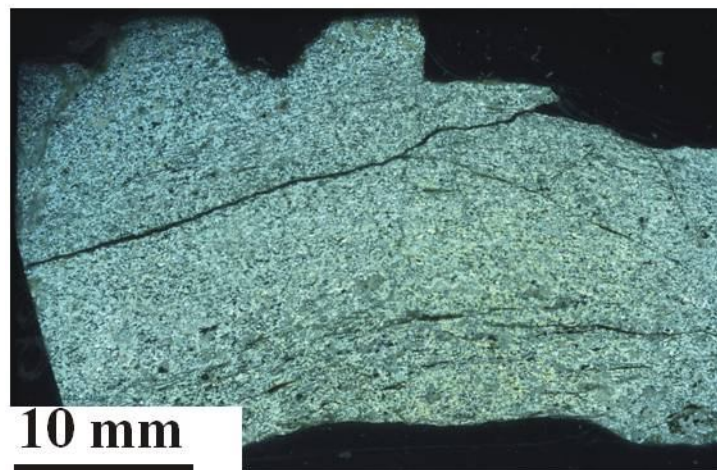


Figure 2: Representative whole thin section of studied sample. The foliation is defined mainly by the parallel alignment of phyllosilicate minerals.

### Sample preparation

A thin section was cut parallel to stretching lineation (Fig. 4) and normal to the foliation, which was then polished using standard mechanical grinding methods. The polished section was then further polished on a polyurethane lap for 2 hours

using a suspension of 0.05  $\mu\text{m}$  colloidal silicon (SYTON) to remove surface damage caused by the initial mechanical polishing. A very thin carbon coat was then added and the edges of the sample were coated with conductive carbon paint to prevent charging during EBSD analysis.

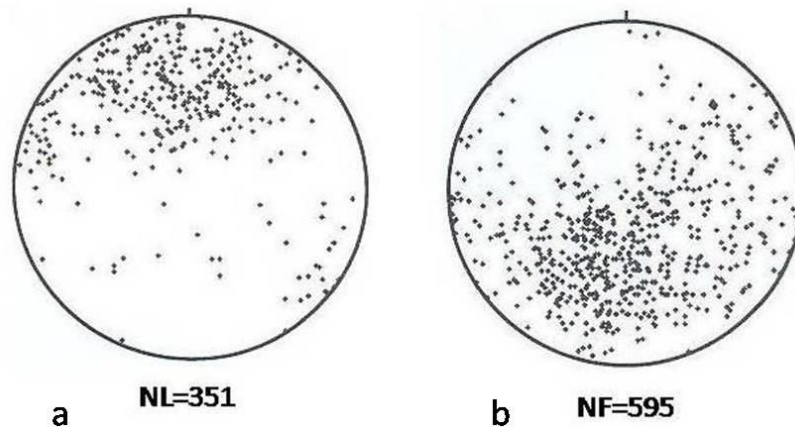


Figure 3: Lineation (a) and foliation (b) fabrics plotted on lower hemisphere equal-area stereographic projections; NL = number of lineation and NF = number of foliation.

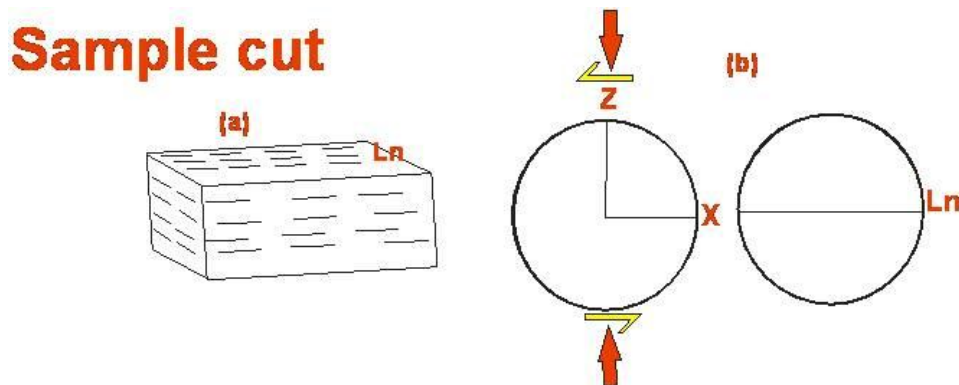


Figure 4: Block diagram shows (a) the geometry of sample and orientation of lineation (Ln); (b) the distribution of XYZ and orientation of Ln are shown on the circle.

### Sample description

The mineral assemblage of the sample comprises quartz (up to 8 0%), muscovite, biotite, feldspar, sillimanite and opaque under optical microscope. The above mineral assemblage could be characterized as a quartz-rich psammite rock. Quartz crystals are up to 3 mm in length, typically inequant in shape. Quartz crystals are more elongated, with grain length ranging between 131 and 543  $\mu\text{m}$  with an average of 233 $\mu\text{m}$ . The high quartz content of the sample means that quartz grains are typically in contact with each other (Fig. 5). Quartz crystals show strong alignment that is parallel to a weak foliation in the rock. Quartz-mica (e.g., muscovite) junctions are straight with the quartzes approximately elongated parallel to this boundary, in comparison to the shorter and more irregular quartz-quartz crystal.

Quartz crystals show patchy undulose extinction. Also, quartz crystals show evidence of sub-grain development and minor grain boundary migration, suggesting they are strained.

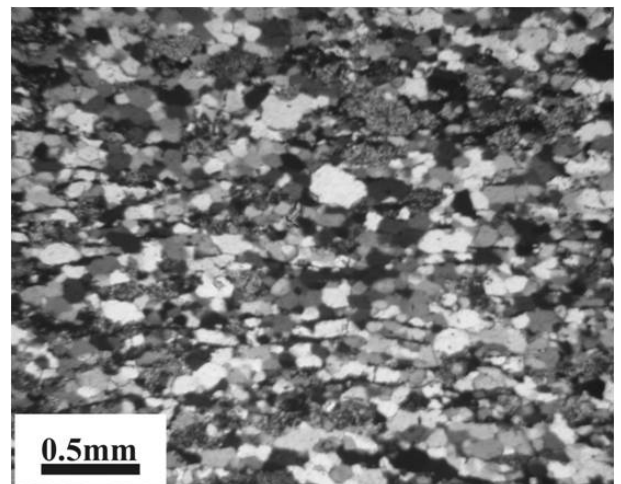


Figure 5: Optical image (crossed polars) of strongly elongated quartz crystals (grey and white); Qtz= quartz.

### EBSD technique

All crystallographic orientations of quartzes were collected by EBSD using a CamScan X500 crystal probe SEM at Liverpool University. This SEM is fitted with a thermionic field emission gun and a FASTRACK stage (see Prior *et al.*, 2002). The

polished specimen surface was inclined at  $20^\circ$  to the incident beam. The accelerating voltage and beam current were 20 kV and  $\sim 5$  nA respectively.

Electron backscatter patterns were processed using CHANNEL+v5 from HKL Technologies (Denmark). The angular resolution of this technique is typically better than  $1^\circ$ . Spatial resolution is  $0.1 \mu\text{m}$ . Data were collected using the

FASTRACK stage to collect onto rectangular grids with  $30 \mu\text{m}$  spacing approximately one point per quartz grain across the whole thin section (Prior *et al.*, 2002). Between four and six bands' diffraction patterns were picked automatically (Fig. 6) using the Hough transform routine in the Channel 5.0 program (see Prior *et al.*, 2002).

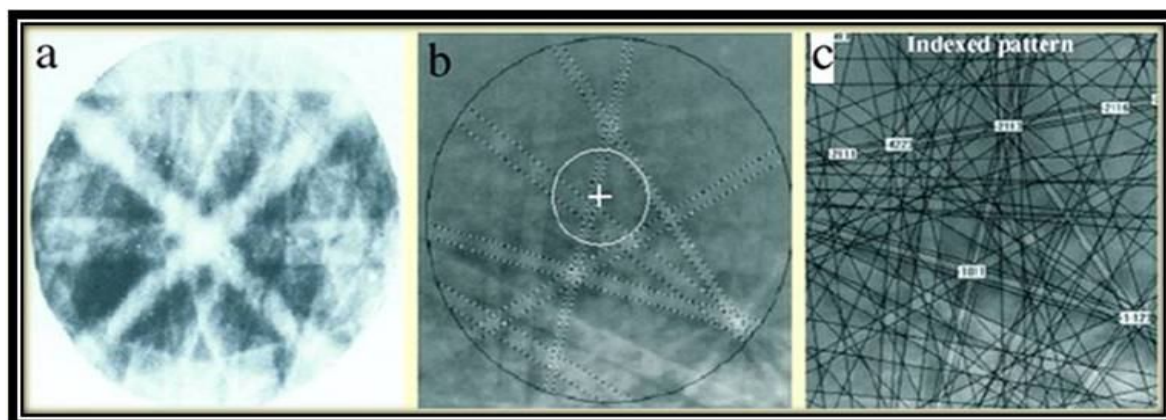


Figure 6: a) Electron channelling pattern from quartz; b) Electron backscattered diffraction (EBSD) pattern of the selected quartz crystal in sample; c) EBSD pattern indexing showing a number of commercial, computer-based systems which store crystal diffraction characteristics in a database.

Euler-angle maps have been post-processed using the Tango utility within Channel+v5 to remove artefacts caused by missing data and local mis-indexing of quartz. Further processing was undertaken to produce data sets for pole-figure plotting in which there is only one point per single grain: a grain defined as having  $>2^\circ$  misorientation with its touching neighbours and being greater than  $20 \mu\text{m}$  for quartz grains. The processed data are plotted as pole figures in the reference frame (XYZ), defined from the specimen schistosity (XY plane) and grain shape elongation (X). The pole figures are oriented with XZ in the drawing plane, which shows that lineation is horizontal (Fig. 4). The quartzes' pole figures are plotted in Y normal to the drawing plane and X horizontal, as in Fig. 7. All pole figures were plotted using the PFch5.exe program published by David Mainprice ([ftp://saphir.dstu.univmontp2.fr/pub/TPHY/david/CareWare\\_Unicef\\_Programs/PC](ftp://saphir.dstu.univmontp2.fr/pub/TPHY/david/CareWare_Unicef_Programs/PC)).

## Results and discussion

The studied sample from north of the RBS (Fig. 1) is characterized by very well-pronounced quartz c-axis [0001] maxima (Fig. 8) near the Y axis (Fig. 4), with a slight tendency to be distributed along a single girdle within the YZ-plane. However, the a-

axes [11 $\bar{2}$ 0] form two small clusters along the margin of the pole figure, and a rather weak fabric asymmetry. The crystallographic orientations of quartz crystals may relate to (i) lattice rotation, (ii) grain boundary migration and (iii) diffusion processes (e.g., Jessell & Bons, 2002; Hirth & Tullis, 1992). Lattice rotation might be caused by dislocation glide, twinning, kinking, rotation recrystallization or grain rotation. These mechanisms can produce strong CPOs in quartz crystals. Hirth and Tullis (1992) have explained that the glide of dislocations on slip planes generally leads to the reorientation of the crystal lattice, which causes a CPO. Jessell and Bons (2002) have suggested that at higher temperatures, many grains will deform, since the critical resolved shear stress of all slip systems reduces with increasing temperature, but at low temperatures, grains tend not to deform at all and tend to be preserved as augen grains.

Previous researchers like Schmid and Casey (1986) infer that quartz-c-axis patterns with a maximum cluster around the Y-axis could be explained by the dominance of prism  $\langle a \rangle$  gliding (Fig. 8) and are typical for medium- to high-grade metamorphic conditions. However, Jessell and Lister (1990) have noted that an asymmetry of

clustering close to the Z-axis in the quartz crystals can be correlated with medium metamorphic temperature. This can be interpreted in terms of

preferred slip on the rhombs, indicating that dislocation creep was the dominant process.

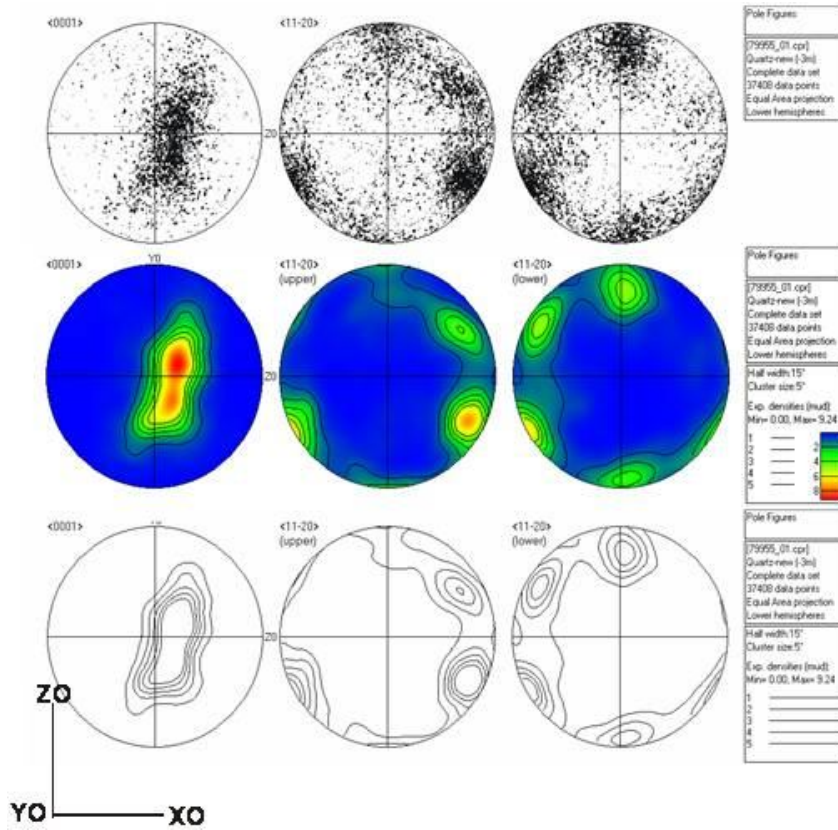


Figure 7: Quartz crystallographic orientations are plotted as pole figures and contour diagrams in  $\langle 0001 \rangle$  and  $\langle 11\bar{2}0 \rangle$  directions in stereonets of lower hemisphere of equal area projection, which were obtained automatically. Kinematic reference is shown as ZO, YO, XO. N = number of grains.

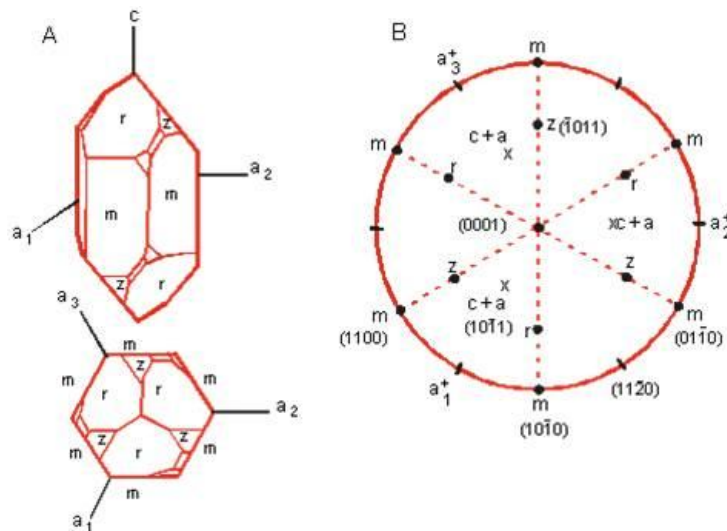


Figure 8: Crystal faces and directions in quartz are showing the most important slip planes and slip directions. A. Crystal morphology with crystallographic axes and faces labelled. Here m indicates the prism planes; r and z indicate the positive and negative rhombohedral planes and the plane normal to c is the basal plane. B. Upper-hemisphere equal-angle projection of the poles to crystallographic planes (dots) and the crystallographic directions (x's) in quartz, oriented as shown in the lower of the two diagrams in part A (slightly modified from Twiss & Moores, 2007).

Therefore, according to Fig. 7, the c-axis fabric of quartz crystals has been interpreted as indicating that prism  $\langle a \rangle$  is the dominant slip system (e.g., Wilson, 1975; Lebit, *et al.*, 2002).

Then, the strong CPOs fabrics of quartz crystals could be characteristic of both high-grade metamorphic conditions and high finite strain. The presence of a CPOs could be explained by dislocation slip. Dislocation usually takes place when movement of lattice defects occurs through the quartz lattice as an intracrystalline deformation

(e.g., Passchier & Trouw, 1996). The dislocation creep mechanism (Fig. 9) is a required condition to produce a quartz c-axis fabric (e.g., Bouchez *et al.*, 1983; Fliervoet *et al.*, 1999). On the other hand, the quartz single cluster c axes distribution's texture is accompanied by sub-grain rotation recrystallization of the deformation mechanism (Bestmann *et al.*, 2011). The asymmetric crossed girdles of an axis can be related to dominating non-coaxial deformation geometry under plane strain conditions.

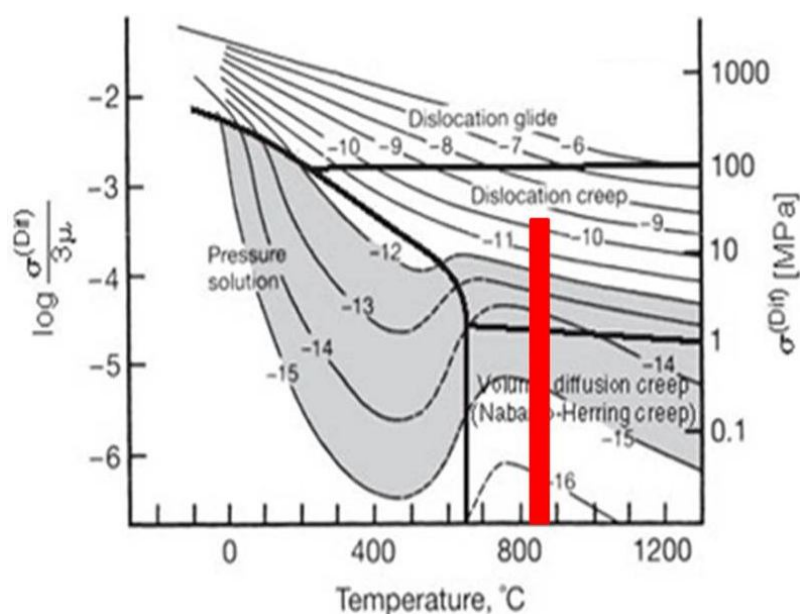


Figure 9: Deformation mechanism map of quartz crystal represents plot of normalized stress (differential stress divided by shear modulus) versus temperature (slightly modified from Twiss & Moores, 2007). Red rectangle shows deformation mechanism of quartzes in studied sample.

## Conclusion

EBSD analysis of quartz crystals in the studied sample shows a distinctive CPO involving a cluster of c-axis orientations close to the inferred intermediate principal strain direction (Y) in the sample. The asymmetric clustering close to the strain ellipsoid Y-axis in the sample can be related to high metamorphic temperature and high finite strain, consistent with heating from the adjacent DCDC during sinistral strike-slip motion on the RBS. The CPO can be explained by the dominance of prism  $\langle a \rangle$  gliding, indicating that dislocation creep was the dominant deformation mechanism.

## References

- Bestmann, M., Pennacchioni, G., Frank, G., Göken, M. and Wall, H., 2011. Pseudotachylite in muscovite-bearing quartzite: Coseismic friction-induced melting and plastic deformation of quartz, *Journal of Structural Geology*, 33: 169-186.
- Bouchez, J. L., Lister, G. S. and Nicolas, A. 1983. Fabric asymmetry and shear sense in movement zones. *Geol. Rdsch*,

## Acknowledgements

The author acknowledges the financial support of the Ministry of Science, Research and Technology and Golestan University of Iran. Furthermore, I appreciate Alan Boyle who gave access to some samples from the north-west Connemara area and discussed the topics presented in this study. I would also like to thank Dave Prior who has operated and maintained EBSD at the University of Liverpool. The paper benefited from the detailed reviews and I wish to express my gratitude to both careful reviewers. I thank E. Ghasemi-Nejad for editorial handling.

- 72: 401-419.
- Boyle, A. P., Dawes, I. P. 1991. Contrasted metamorphic and structural evolutions across a major ductile/brittle displacement zone in NW Connemara, western Ireland, *Geologische Rundschau*, 80(2): 459-480.
- Brunel, M., 1980. Quartz fabrics in shear-zone mylonites: evidence for a major imprint due to late strain increments. *Tectonophysics*, 64: 33-44.
- Chew, D.M., 2003. Structural and stratigraphic relationships across the continuation of the Highland Boundary Fault in western Ireland. *Geol. Mag.*, 140: 73-85.
- Clift, P. D., Dewey, J. F., Draut, A. E., Chew, D. M., Mange, M., Ryan, P. D., 2004. Rapid tectonic exhumation, detachment faulting and orogenic collapse in the Caledonides of western Ireland, *Tectonophysics*, 384: 91-113.
- Fliervoet, T. F. and White, S. H. 1995. Quartz deformation in a very fine grained quartzo-feldspathic mylonite: a lack of evidence for dominant grain boundary sliding deformation. *Journal of Structural Geology*, 17: 1095-1109.
- Friedrich, A. M., Bowring, S. A., Martin, M.W., Hodges, K. V., 1999a. Short-lived continental magmatic arc at Connemara, western Irish Caledonides: implications for the age of the Gramscian Orogeny. *Geology*, 27: 27-30.
- Friedrich, A. M., Hodges, K.V., Bowring, S.A., Martin, M.W., 1999b. Geochronological constraints on the magmatic, metamorphic, and thermal evolution of the Connemara Caledonides, western Ireland. *J. Geol. Soc. (Lond.)*, 156: 1217-1230.
- Hirth G. and Tullis J., 1992. Dislocation creep regimes in quartz aggregates. *Journal of Structural Geology*. 14: 145-159.
- Jessell, M.W., Lister, G.S., 1990. Temperature dependence of quartz fabrics. In: Knipe, R.J., Rutter, E.H. (Eds.), *Deformation Mechanisms, Rheology and Tectonics*. Geological Society Special Publication, 54: 353-362.
- Jessell M.W. & Bons, P.D., 2002. The numerical simulation of microstructure. In: de Meer, S., Drury, M.R., de Bresser, J.H.P. & Pennock, G.M. (eds.) *Deformation Mechanisms, Rheology and Tectonics: Current Status and Future Perspectives*. Geol. Soc, London, Spec. Publ., 200: 1137-147.
- Jiang, Z., Prior, D.J. & Wheeler, J. 2000. Albite crystallographic preferred orientation and grain misorientation distribution in a low-grade mylonite: implications for granular flow. *Journal of Structural Geology*, 22: 1663-1674.
- Klaper, E.M., 1988. Quartz c-axis fabric development and largescale post-nappe folding (Wandfluhhorn fold, Penninic Nappes). *Journal of Structural Geology*, 10: 795-802.
- Law, R. D. 1986. Relationship between strain and quartz crystallographic fabrics in the Roche Maurice quartzites of Plougastel, western Brittany. *Journal of Structural Geology*, 8: 493-515.
- Law, R. D. 1990. Crystallographic fabrics: a selective review of their applications to research in structural geology. In: Knipe, R.J. and Rutter, E.H., Editors, 1990. *Deformation Mechanisms, Rheology and Tectonics*, Geological Society Special Publication. 54: 335-352.
- Law, R., Casey, M., Knipe, R.J., 1986. Kinematic and tectonic significance of microstructures and crystallographic fabrics within quartz mylonites from Assynt and Eriboll regions of the Moine thrust zone NW Scotland. *Transactions of the Royal Society of Edinburgh: Earth Sciences*, 77: 99-123.
- Lebit, H., Klaper, E. M., Lueneburg, C. M. 2002. Fold-controlled quartz textures in the Pennine Mischabel backfold near Zermatt, Switzerland. *Tectonophysics*, 359: 1-28.
- Lister, G.S., 1977. Crossed girdle c-axis fabrics in quartzites plastically deformed by plane strain and progressive simple shear. *Tectonophysics*, 39: 51-54.
- MacCready, T., 1996. Misalignment of quartz c-axis fabrics and lineations due to oblique final strain increments in the Ruby Mountains core complex, Nevada. *Journal of Structural Geology*, 18 (6): 765-776.
- Mancktelow, N.S., Pennacchioni, G., 2004. Microstructures of quartz mylonites: the importance of grain boundary fluids. *Journal of Structural Geology*. 26: 47-69.
- Passchier, C. W. & Trouw, R. A. J. 1996. *Microtectonics*. Springer-Verlog Berlin Heidelberg.
- Rahimi-Chakdel, A., Boyle, A. P., Prior, D. J. 2006. Quartz deformation mechanisms during Barovian metamorphism: Implication from crystallographic orientation of different generation of quartz in Pelites. *Tectonophysics*, 427: 15-34.
- Schmid, S. M. & Casey, M. 1986. Complete fabric analysis of some commonly observed quartz c-axis patterns. In: *Minerals and rock deformation: Laboratory studies*, The Patterson Volume (edited by Hobbs BE & Heard HC), American Geophysical Union, Geophysical Monograph, 36: 263-286.
- Spry, A. 1969. *Metamorphic Textures*. Pergamon Press, Oxford.
- Tullis, J. 1977. Preferred orientation of quartz produced by slip during plane strain. *Tectonophysics*, 39: 87-102.
- Twiss, R. J. and Moores, E. M., 2007. *Structural geology*. Freeman and Company New York, Second edition.
- Power, S.E., Ryan, P.D., Feely, M., 2001. Fluid inclusion studies on the late structural history of the Connemara Dalradian, western Ireland. *GSA* 33 (6), A448 (Abstr. with prog.).
- Prior, D.J., Wheeler, J., Peruzzo, L., Spiess, R., Storey, C., 2002. Some garnet microstructures: an illustration of the potential of orientation maps and misorientation analysis in microstructural studies. *Journal of Structural Geology*. 24: 999-1011.
- Unzog, W. and Kurz, W. 2000. Progressive development of lattice preferred orientations (LPOs) of naturally deformed

- quartz within a transpressional collision zone (Panafrican Orogen in the Eastern Desert of Egypt), *Journal of Structural Geology*, 22: 1827-1835.
- Wellings, S.A., 1998. Timing of deformation associated with the syn-tectonic Dawros–Currywongaun–Doughruagh Complex, NW Connemara, western Ireland. *J. Geol. Soc. (Lond.)* 155: 25–37.
- Wenk, H. R. 1985. Preferred Orientation in Deformed Metals and Rocks: An Introduction to Modern Texture Analysis. Academic Press, London, 610.
- Williams, D.M., Rice, A.H.N., 1989. Low-angle extensional faulting and the emplacement of the Connemara Dalradian, Ireland. *Tectonics*, 8: 427–428.
- Yardley, B. W. D., Vine, F. J., Baldwin, C. T., 1982. The plate tectonic setting of NW Britain and Ireland in Late Cambrian and Early Ordovician times. *J. Geol. Soc. (Lond.)*, 139: 455–463.